

Broadband Millimeter-Wave Microstrip Comb-Line Antenna Using Corporate Feeding System with Center-Connecting

Atsushi KUNITA[†], *Student Member*, Kunio SAKAKIBARA^{†a)}, *Senior Member*, Kazuyuki SEO^{††b)}, *Member*, Nobuyoshi KIKUMA[†], *Fellow*, and Hiroshi HIRAYAMA[†], *Member*

SUMMARY A broadband microstrip comb-line antenna using a corporate feeding system was developed. The antenna was composed of four colinearly-arranged comb-line antennas with traveling-wave excitation fed by a parallel-feeding circuit of tournament configuration. The total phase deviation due to frequency change became one fourth of the ordinary series feeding from the end of the antenna. Furthermore, the terminations of the inner two comb-lines were connected at the overall center of the developed antenna. Therefore, the narrowband matching elements are not necessary and the amplitude deviation of the aperture distribution for input from one side due to frequency change is compensated by deviation for input from the other side. Broad bandwidth can be expected by using the proposed configuration. The proposed antenna was designed at 76.5 GHz. The effect of the proposed feeding-circuit for broadband operation was confirmed by comparing the measured performances of the antennas fed by other feeding circuits; the end feeding, the center feeding and the ordinary corporate feeding. The bandwidth of the proposed corporate feeding antenna with the center connecting was approximately 14% and 7% wider than the antennas of the center feeding and of the ordinary corporate feeding, respectively.

key words: millimeter-wave, microstrip antenna, array antenna

1. Introduction

Broadband systems have been expected in the millimeter-wave band for UWB radars of sensing applications [1] and for high-speed wireless HD transmission systems of wireless communication applications [2]. The beam-scanning functions are attractive to cover wide angular-range with high gain. The electrical beam-scanning systems such as phased arrays and digital beam forming (DBF) systems were proposed for these applications, because the cost of RF devices dropped after the recent commercialization of the automotive radar systems in market from some motor companies. Horizontal beam-scanning is one of the possible functions to detect the directions of the radar targets on the road and to catch signals from the multiple-channel environment in houses and offices. Some vertically-directed one-dimensional arrays are arranged in horizontal direction to scan the beam in the azimuth plane. Broadband vertically-long planar antennas are required for sub-arrays of electrical

beam-scanning systems.

We have developed microstrip comb-line antennas in the millimeter-wave band, which can be applied to these systems [3]. The antennas operate in traveling-wave excitation. However, the bandwidth of directivity at the fixed direction is narrower due to the beam squint from the beam direction at the design frequency. The directivity reduction can be decreased by using a combination of the tournament configuration for parallel feeding and the traveling-wave excitation for series feeding. Several research organizations have already developed corporate feeding systems for slotted waveguide array antennas [4], [5]. We proposed broadband microstrip comb-line antennas fed by the waveguide corporate feeding system in this paper. This waveguide corporate feeding system can be formed in the existing back metal layer with the waveguide connecting the antennas and the microwave circuits. Two colinearly-arranged comb-line antennas were fed at their middles from the parallel-feeding circuit of tournament configuration, that is four end-feeding comb-line antennas fed by a waveguide two-way power divider. Furthermore, the terminations of the inner two comb-lines are connected at the overall center of the developed antenna. Therefore, the narrowband matching elements are not necessary there and the amplitude deviation of the aperture distribution for the input from one side due to frequency change is compensated by the deviation for the input from the otherside. Broadband performance is expected by using the proposed structure. The proposed antenna was designed and the performance was confirmed by simulations and experiments in the millimeter-wave band.

2. Variation of Phase Distribution Depending on the Feeding Systems

The feeding systems of the linearly arranged microstrip comb-line antennas consist of various combinations of a tournament configuration for parallel feeding and a traveling-wave excitation for series feeding as shown in Fig. 1. The bandwidth of the directivity toward the perpendicular direction limited by the phase taper of the aperture distribution depends on the parallel number of the antenna. The end-feeding comb-line antenna shown in Fig. 1(a) performs narrow frequency bandwidth, because the beam squint causes reduction of directivity at the perpendicular direction. However, the bandwidth increases, as increasing the parallel number of the comb-line antennas di-

Manuscript received March 6, 2011.

Manuscript revised July 7, 2011.

[†]The authors are with the Department of Computer Science and Engineering, Nagoya Institute of Technology, Nagoya-shi, 466-8555 Japan.

^{††}The author is with Development 2nd Dep., Business Creative Division NIPPON PILLAR PACKING CO., LTD., Sanda-shi, 669-1333 Japan.

a) E-mail: sakaki@nitech.ac.jp

b) E-mail: kazuyuki.seo@pillar.co.jp

DOI: 10.1587/transcom.E95.B.41

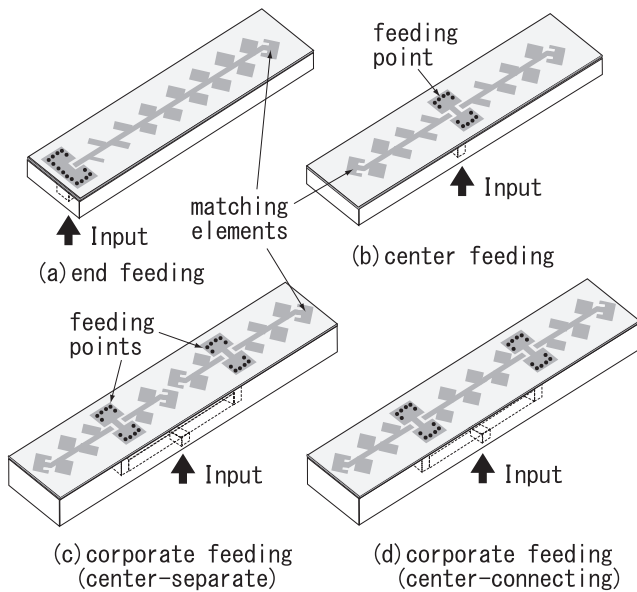


Fig. 1 Microstrip comb-line antennas with various feeding numbers and points.

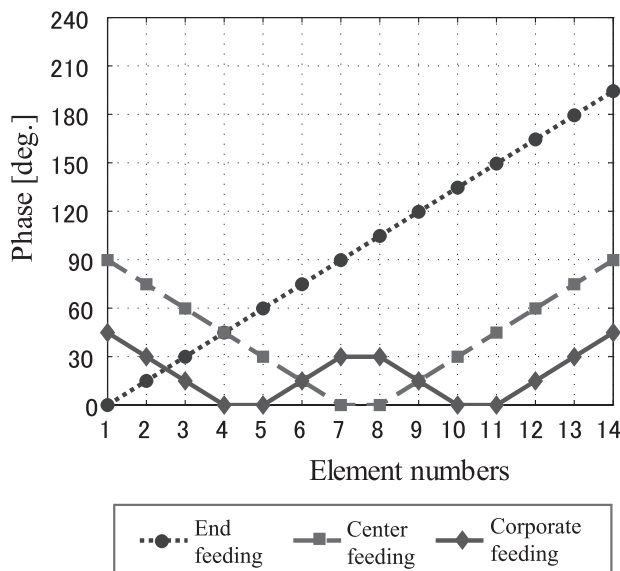


Fig. 2 Aperture phase distributions depending on the feeding numbers and points.

vided by the feeding points on the substrate as shown in Figs. 1(b), (c) and (d).

Figure 2 shows the aperture phase tapers due to the change of the guided wavelength when the operating frequency shifts by 3 GHz lower than 76.5 GHz of the design frequency. The maximum phase deviation is inversely proportional to the parallel number of feeding. The phase deviation of the center feeding (b) becomes one half of the end feeding (a), furthermore, the phase deviations of the corporate feedings (c) and (d) become one fourth of the end feeding (a). The difference between the feeding systems (c) and (d) is the amplitude distributions, which will be mentioned in the next section, while the frequency dependen-

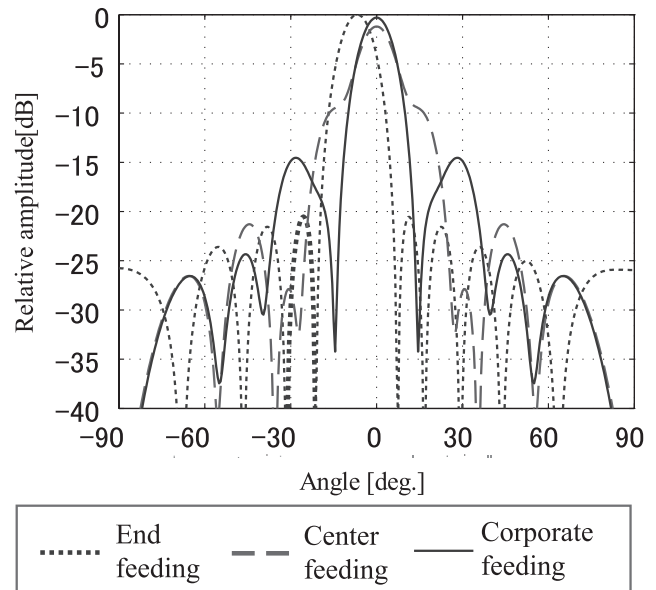


Fig. 3 Array factors depending on the feeding numbers and points.

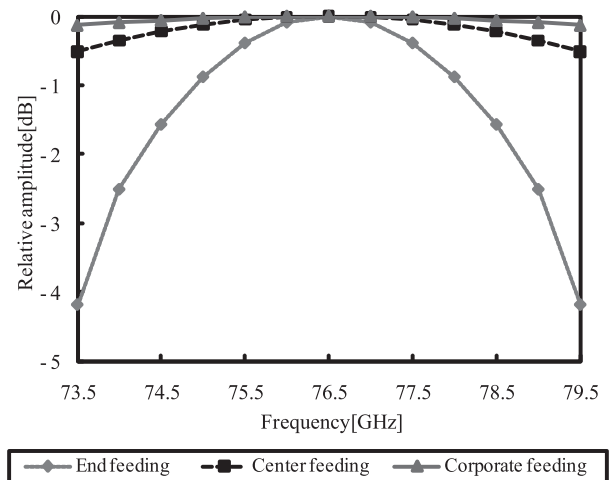


Fig. 4 Calculated frequency dependency for directivity of array factor.

cies of the phase distributions are almost the same essentially. The directivity of the end-feeding antenna (a) at the perpendicular direction dropped by approximately 3 dB due to the beam squint, when frequency changes by 3 GHz, as shown in Fig. 3. The beam directions of the center-feeding antenna and the corporate feeding antennas are stable at the perpendicular direction due to their symmetrical structures, although the sidelobe levels grew up and the directivities dropped slightly. Figure 4 shows the frequency dependency of the antenna directivity. The directivity of the end-feeding antenna dropped rapidly when frequency changed. The bandwidth extended when the number of the feeding points increased. The corporate feeding system is effective to extend the bandwidth of the directivity. The advantage of the proposed corporate feeding system (d) in the bandwidth of the amplitude distribution will be presented in the next

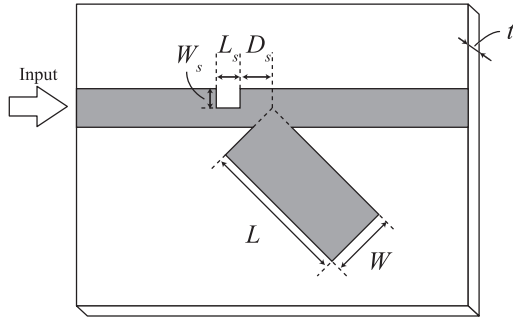


Fig. 5 Radiating element with reflection-canceling slit structure.

section.

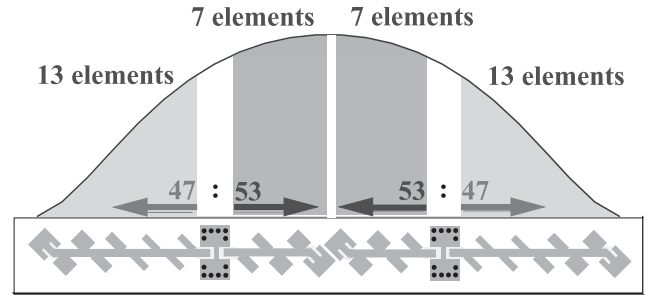
3. Configuration and Design of the Comb-Line Antennas Fed from the Corporate Feeding Systems

Two antennas with the different corporate-feeding systems shown in Figs. 1(c) and (d) were designed at 76.5 GHz. The details about the feeding systems were explained in the following Sects. 3.1 and 3.2.

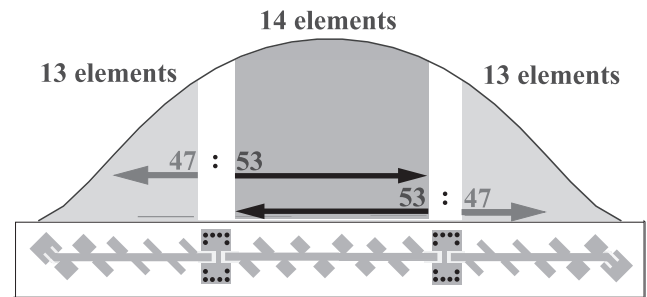
The microstrip comb-line antennas are printed on the dielectric substrate (Fluoro-carbon resin film, thickness $t = 0.127$ mm, relative dielectric constant $\epsilon_r = 2.2$ and loss tangent $\tan\delta = 0.001$) backed with a ground plane. Several rectangular radiating elements are directly attached to a straight feeding-line, which results in comb-line structure. The radiating elements are inclined 45 degrees from the feeding microstrip line for the polarization requirement of the automotive radar systems. Each radiating element equips a reflection-canceling slit structure, as shown in Fig. 5, to improve the reflection characteristics and the design accuracy of the radiation pattern [3]. The resonant length of the radiating element is approximately identical to a half guided wavelength. The width of the feeding line is 0.30 mm, whose characteristic impedance is 60Ω . The coupling power of the radiating element is controlled by the width of the element. Large power radiates from a wide element. The element spacing is approximately a half guided-wavelength, so that all elements on the both sides of the microstrip line are excited in phase. A matching element is connected at the termination of the feeding line to radiate all the residual power in phase. The ordinary microstrip patch antennas are used for the matching elements. Four end-feeding microstrip comb-line antennas are colinearly arranged and are fed by the corporate waveguide feeding circuit from the back as shown in Fig. 1(c). To improve the bandwidth of the aperture amplitude distribution, the inner feeding lines are connected at their terminations as shown in Fig. 1(d). The performance of the center-connecting antenna was compared with that of the center-separate antenna.

3.1 Center-Separate Antenna Fed from Corporate-Feeding System

Four colinearly-located end-feeding comb-line antennas are



(a) Center-separate comb-line antenna



(b) Center-connecting comb-line antenna

Fig. 6 Radiation assignment on the apertures of comb-line antennas for Taylor distributions.

fed from the corporate feeding system as shown in Fig. 1(c). The input power is divided equally by the two-way waveguide power-divider located in the lower metal-layer under the substrate. Both the waveguide output ports are connected to the two-way microstrip-to-waveguide transitions at the middle of the two microstrip comb-line antennas, each one of which consists of two end-feeding comb-line antennas. The coupling powers of all the radiating elements are controlled by the width of the elements to obtain Taylor distribution on the aperture as shown in Fig. 6(a). The required aperture distributions were different between the inner and the outer end-feeding comb-line antennas. Therefore, the designs for the inner and the outer comb-line antennas were different, consequently. The numbers of the radiating elements were chosen to be 7 and 13 of the inner and outer antennas, respectively, so that total radiation powers of them becomes comparable. However, the total radiation powers between the inner and the outer antennas are still different. The microstrip-to-waveguide transition with the asymmetrical dividing ratio 53:47 was developed, as mentioned in Sect. 3.3.

The dimensions of the radiating elements shown in Fig. 5 at the left half of the center-separate and the center-connecting antennas are indicated in Fig. 7. The outer 13 elements are common parameters in the two antennas. The coupling powers of the elements at both the inner and the outer sides increase, as the elements being away from the input port between the element numbers 13 and 14. Both

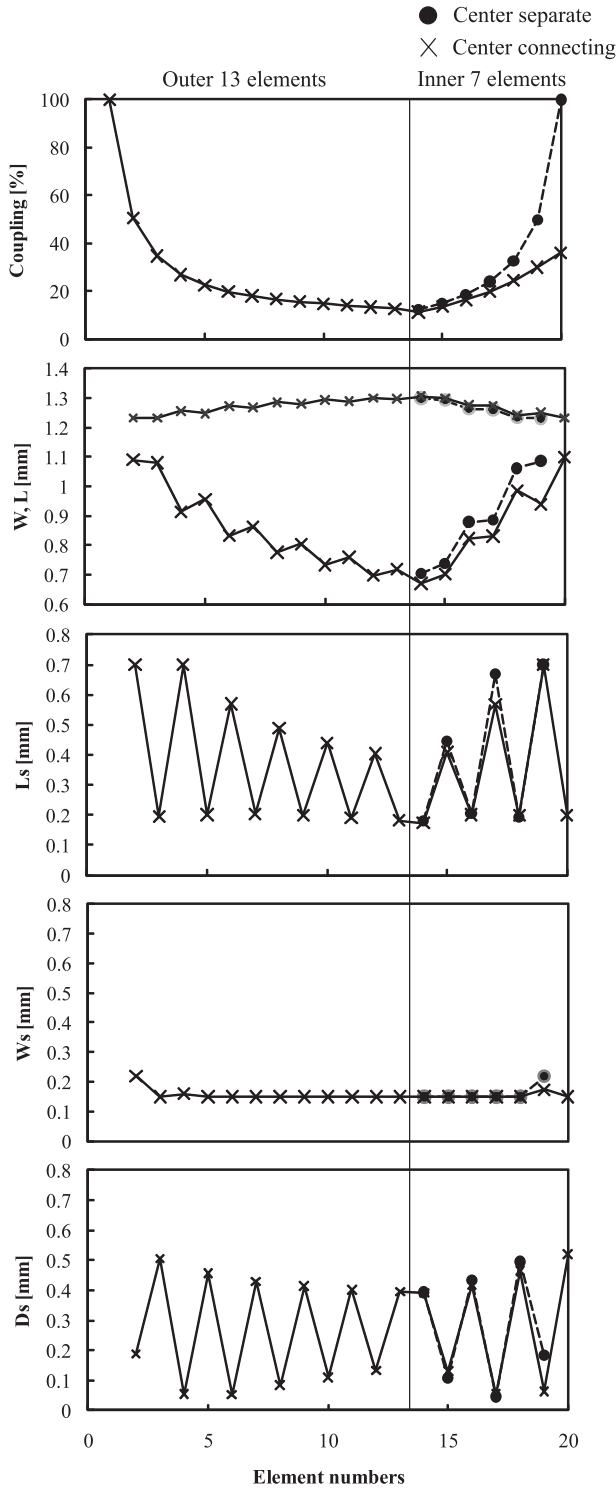


Fig. 7 Geometrical dimensions of the radiating elements in the center-separate and the center-connecting comb-line antennas.

the inner 7 elements and the outer 13 elements are terminated by the matching elements with coupling power 100% in the center-separate antenna. The radiation characteristics are different between the elements at the opposite sides of the feeding line. Therefore, the element and the slit dimen-

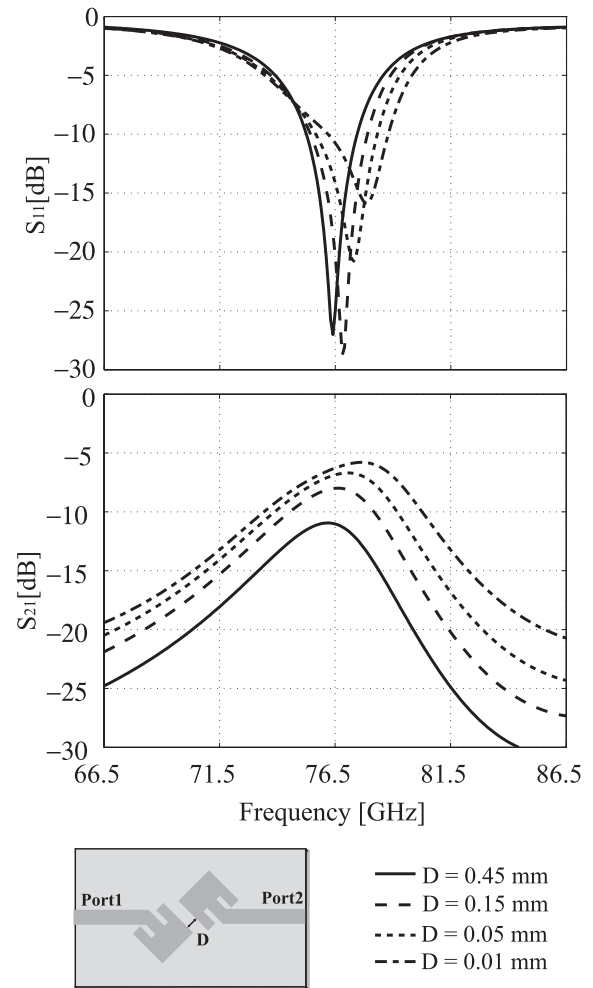


Fig. 8 Effect of the mutual coupling between the matching elements in S_{11} and S_{21} .

sions vary alternately.

3.2 Center-Connecting Antenna Fed from Corporate-Feeding System

The bandwidth of the matching element is quite narrow. Therefore, the shift of the resonant frequency due to the mutual coupling between the closely located matching elements or the fabrication errors in the etching process could cause increasing the return loss and degrading the radiation pattern. Figure 8 shows the effect of the mutual coupling between the matching elements in S_{11} and S_{21} . For the low sidelobe design in the radiation pattern, the spacing D between the matching elements is designed to be small. As the spacing D decreasing, the effect of the mutual coupling increases. Thus, the resonant frequency shifts higher in S_{11} and the return loss increases. At the same time, as S_{21} increases, the radiations from the elements fed from the other side transition could increase, which could degrade the radiation characteristics. Therefore, we propose to remove the matching elements at the antenna center and to connect the

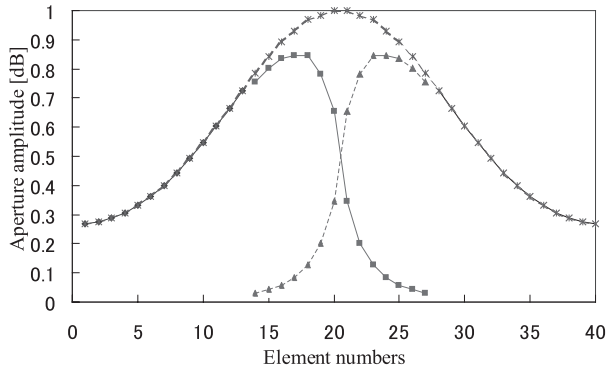


Fig. 9 Total radiation and radiation when feeding from each transition. (square: fed from left transition, triangle: fed from right transition, cross: total radiation)

lines as shown in Fig. 1(d).

The radiation assignment of the center-connecting antenna is almost the same with that of the center-separate antenna in the design. Input powers from both transitions are mixed in the inner microstrip line as shown in Fig. 6(b). The most input power into the inner comb-line antenna from one transition radiates from the first half of the inner comb-line antenna. However, some residual power radiates from the second half of the inner comb-line antenna which is identical to the first half for the input from the opposite transition. The total radiation from one element is sum of radiations fed from both two transitions. The spacing between the two center elements is designed for the radiations to be in phase. The aperture distributions by the total radiation and by the radiations from the elements fed from each transition are indicated in Fig. 9. Both the outer 13-element arrays are fed from each transition. On the other hand, the inner 14-element array is fed from both transitions. To realize Taylor distribution of the total radiation, the power dividing ratio of the transitions is designed to be 53:47 as well as the center-separate antenna, and all the radiating elements are designed including the radiation fed from the opposite transition. From Fig. 7, the coupling power is assigned not very large at the inner part of the center-connecting antenna, because the elements are fed from both transitions.

3.3 Microstrip-to-Waveguide Transition for Asymmetrical Dividing Ratio

Planar microstrip-to-waveguide transitions for symmetrical dividing ratio have been developed [6]–[8]. In this work, a transition with asymmetrical dividing ratio was developed for the feeding circuit of the corporate feeding systems as shown in Fig. 10. Two microstrip lines are inserted as probes into the upper ground plane from both broad-walls of the waveguide. A patch is located at the center of the aperture on the lower plane of the substrate along with the waveguide cross-section. The patch current excited from the waveguide couples to the probes of the microstrip lines. The coupling ratio can be controlled by the difference between the insertion lengths of the probes as shown in Fig. 11. The coupling

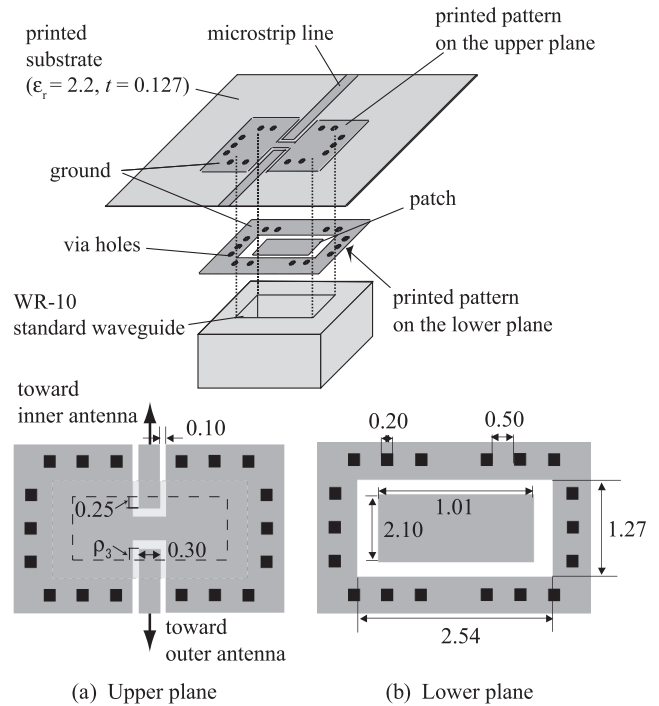


Fig. 10 Microstrip-to-waveguide transition for asymmetric power-dividing ratio. Dimensions are in [mm].

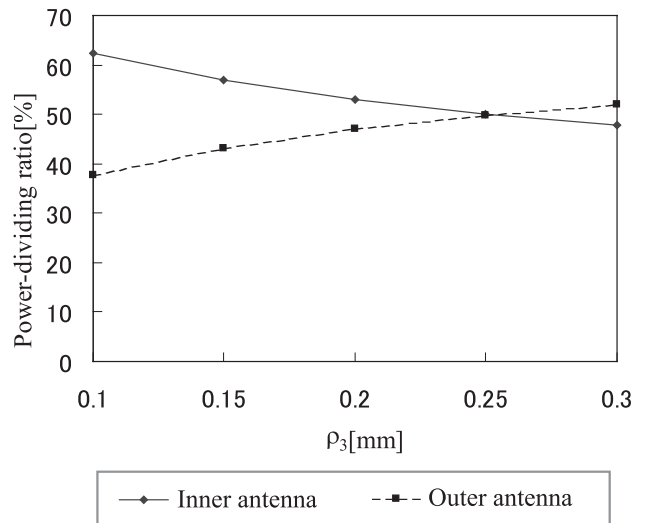


Fig. 11 Power dividing ratio depending on the overlap length of probe with patch.

ratio changes from 62:38 to 49:51, when the overlap length of the probes to the outer antennas on the patch changes from 0.1 to 0.3 mm, while the overlap length of the probes to the inner antennas is fixed to 0.25 mm. In this design, overlap lengths of the probes to the inner and the outer antennas on the patch are 0.25 and 0.20 mm, respectively. Phase difference due to the asymmetrical structure is compensated by spacings between the first radiating element and the transition at both ports.

The four end-feeding comb-line antennas are fed

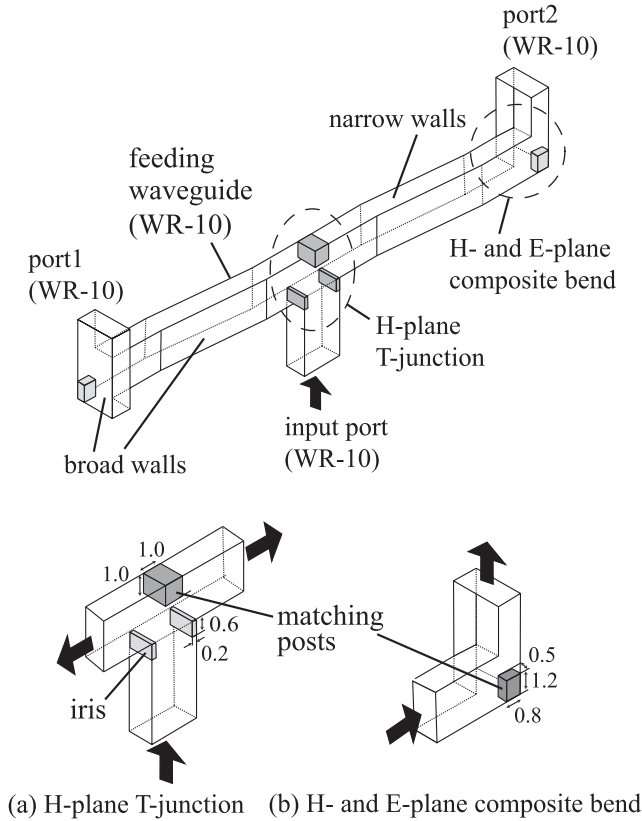


Fig. 12 Feeding circuit of the WR-10 waveguide (2.54×1.27) with H-plane T-junction and H- and E-plane composite bends. Dimensions are in [mm].

through the two asymmetrical transitions from the waveguide feeding circuit composed of a H-plane T-junction and two H- and E-plane composite bends as shown in Fig. 12 [5]. The structure of the waveguide feeding circuit is complicated to use for microstrip antennas. However, this waveguide circuit can be embedded in the metal base of the sensor unit including RF and DSP packages with waveguides to connect the sub-array antennas and RF package.

4. Center-Connecting Antenna Fed from Both Ends

The proposed center-connecting antenna fed from corporate-feeding system was composed of two outer end-feeding antennas and an inner antenna fed from both ends. To demonstrate advantages for bandwidth of the center-connecting feeding system, the performance of the center-connecting antenna shown in Fig. 13(b) was compared with the center-separate antenna shown in Fig. 13(a) by simulations and experiments.

A printed substrate was set on the metal base which accommodate the waveguide feeding circuit mentioned in Sect. 3.3. Whole layer structures were screwed together. The divided powers from the waveguide feeding circuit were supplied to the microstrip antenna from the both sides through the planar microstrip-to-waveguide transition with only one microstrip port [9]. Two comb-line antennas

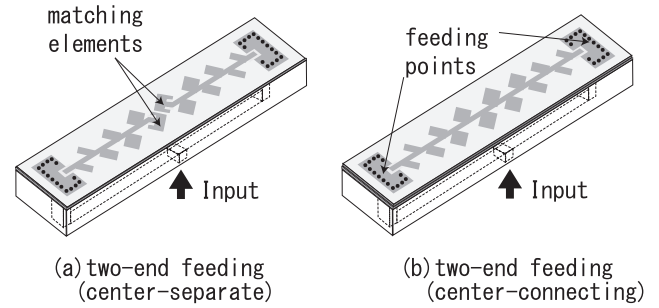


Fig. 13 Two-end feeding antennas.

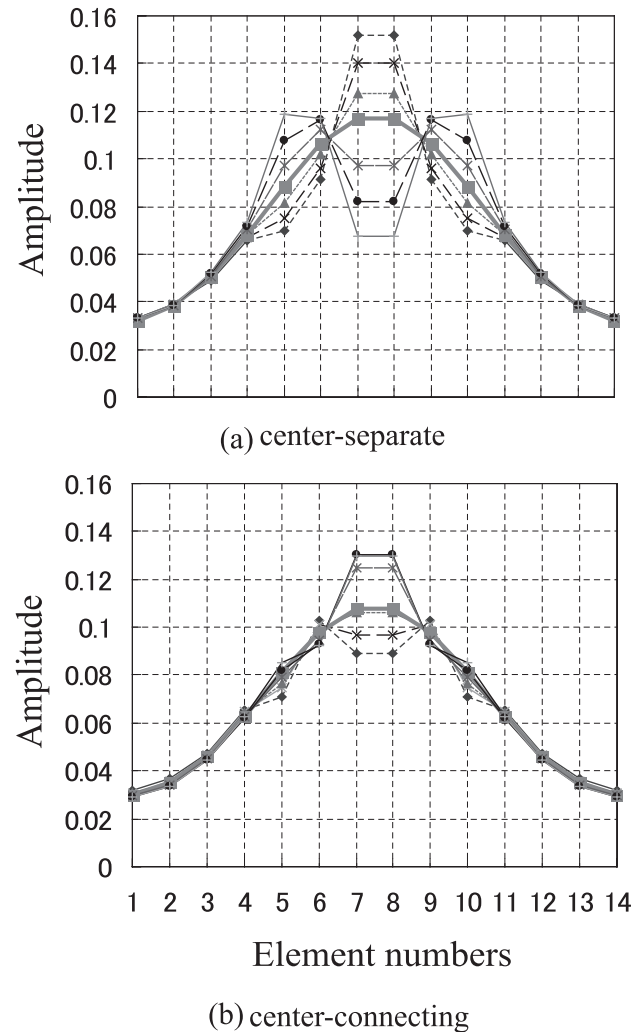


Fig. 14 Frequency dependencies of the aperture distributions.

are fed from the two transitions and are terminated by the closely located matching elements at the center of the center-separate antenna. On the other hand of the center-connecting antenna, the narrowband matching elements are

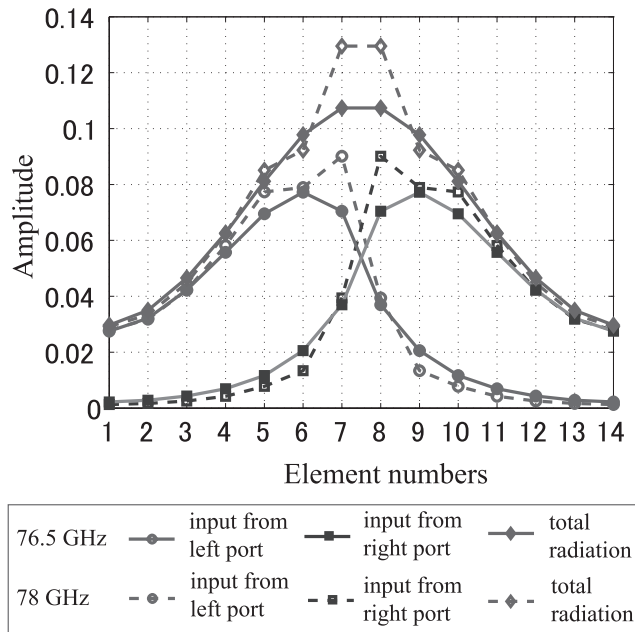
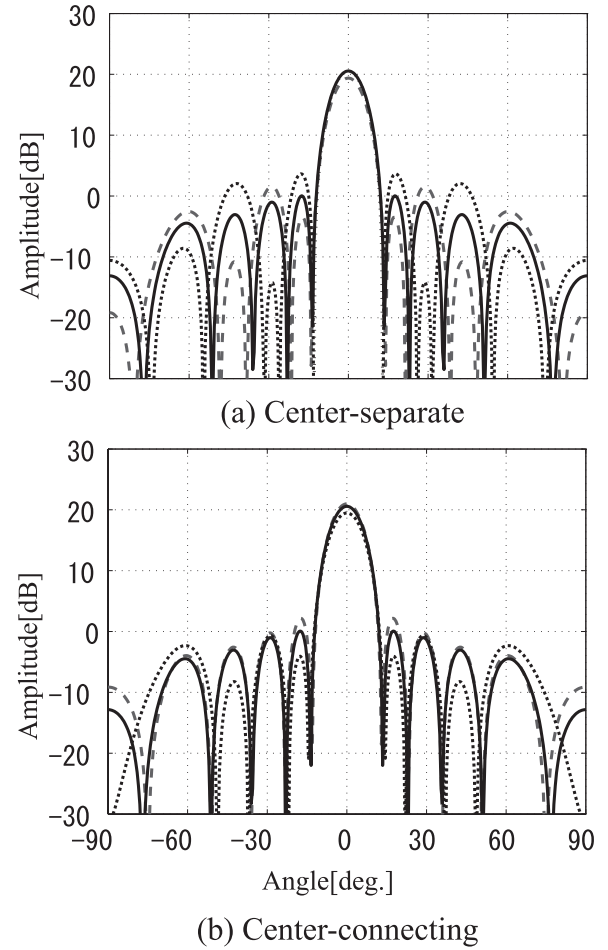


Fig. 15 Radiation distributions on the aperture input from each port and both ports for the design frequency 76.5 GHz and 78 GHz.

not used and the feeding lines are connected at the antenna center. The most power radiates from the first half of the antenna. Some residual power transmits into the second half of the antenna. The amplitude deviation of the aperture distribution for the input from one side is compensated by the deviation for the input from the other side. For example, in some cases, when the radiation from the element decreases due to frequency changes or fabrication errors, the transmission power into the second half of the feeding line increases. Therefore, the radiation from the first half of the antenna fed from the opposite transition also increases. Consequently, total radiation input from both ports changes smaller than center-separate antenna. Broadband and stable performance from fabrication errors are expected by using the proposed structure.

The frequency dependency of the aperture distribution was investigated for the center-separate and the center-connecting antennas. The aperture distributions of these antennas for the different frequencies were indicated in Fig. 14. When the operating frequency changes to lower, the radiation from the elements of the center-separate antenna decreases and the radiation from the matching elements increases. On the other hand, when frequency change to higher, the radiation from the elements increases and the radiation from the matching elements decreases. Such frequency dependency was suppressed by using the center-connecting antenna, because the change of radiation was compensated by the input from the opposite port. Figure 15 shows the radiation distributions on the aperture, when input from each port and both ports at the design frequency 76.5 GHz and at the shift frequency 78 GHz. When frequency changes to higher, radiations for the input from the



--- 75 GHz — 76.5 GHz 78 GHz

Fig. 16 Frequency dependency of the array factors of two-end feeding antennas.

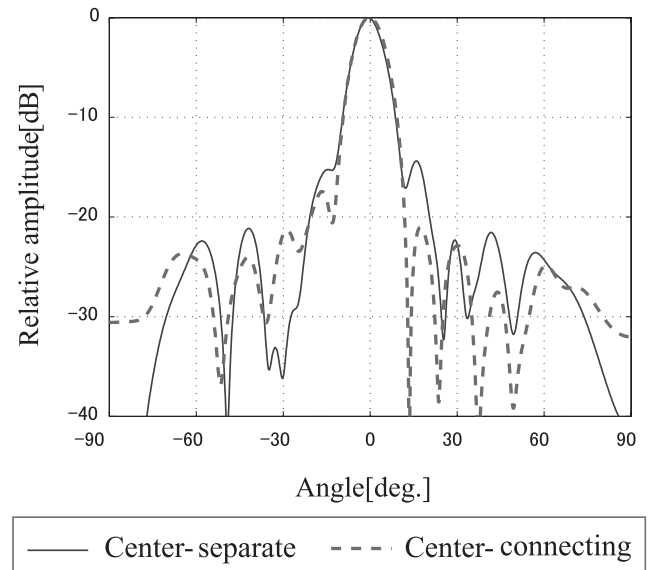


Fig. 17 Measured radiation patterns of the two-end feeding antennas at 78 GHz.

left port increases at the left side and decreases at the right side, while the opposite is equally true. Consequently, the aperture distribution for the sum of the input from both ports are almost stable. Therefore, radiation pattern is also stable for frequency change. Figure 16 shows the array factors calculated from the aperture distributions shown in Fig. 14. The sidelobe levels of the center-separate antenna grow by 3.5 dB when the frequency changes by 1.5 GHz. On the other hand, the sidelobe levels of the center-connecting antenna grow only by 2.1 dB. We fabricated the antennas to compare the performances. Figure 17 shows the measured radiation patterns at 78 GHz. The sidelobe levels of the center-connecting antenna are 2.4 dB lower than the center separate antenna, so we confirmed the advantage of the proposed feeding system of the center-connecting.

5. Experiments

The proposed microstrip comb-line antenna was fabricated for experiments as shown in Fig. 18. The printed substrate was set on the aluminum base-plate in which the waveguide feeding circuit was accommodated. They were all screwed together.

The measured radiation patterns of the center-separate

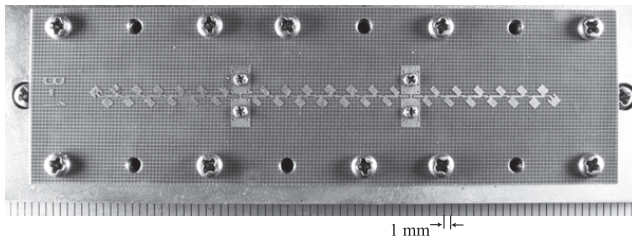


Fig. 18 Photograph of the fabricated center-connecting antenna.

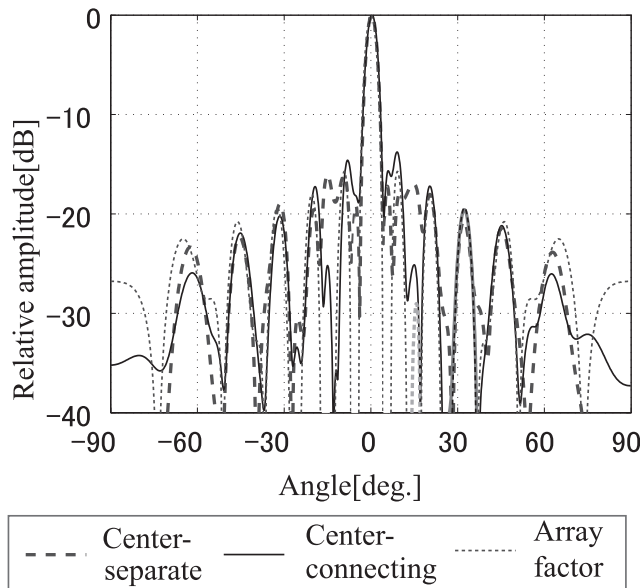


Fig. 19 Measured radiation patterns at the design frequency (76.5 GHz).

and the center-connecting antennas at 76.5 GHz are shown in Fig. 19 with the array factor for reference. The symmetrical radiation patterns were obtained for both antennas. The sidelobe levels were increased to approximately -15 dB, although the design sidelobe level is -20 dB. This is because the blank areas with no radiating element exist around the microstrip-to-waveguide transition. Figures 20 and 21 show simulated and measured radiation patterns, respectively, of the center-separate and center-connecting antennas at 78 GHz. The effect for sidelobe suppression became smaller than the two-end feeding antenna in the previous section, because the two outer antennas are common to the center-separate and the center-connecting antennas. However, the effect was still observed in the simulated and measured results.

Measured relative gain is shown in Fig. 22 to com-

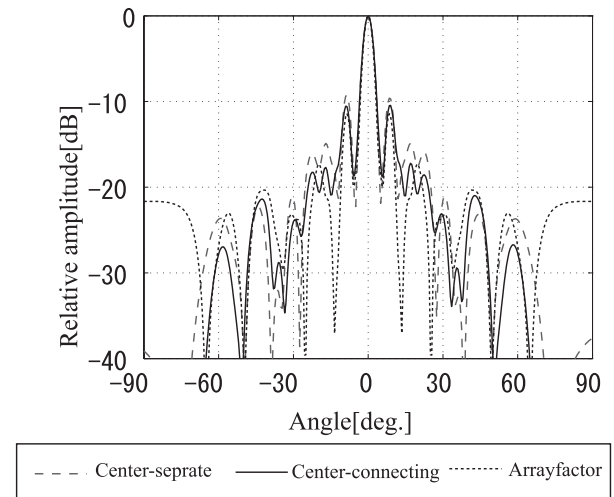


Fig. 20 Simulated radiation patterns at 78 GHz.

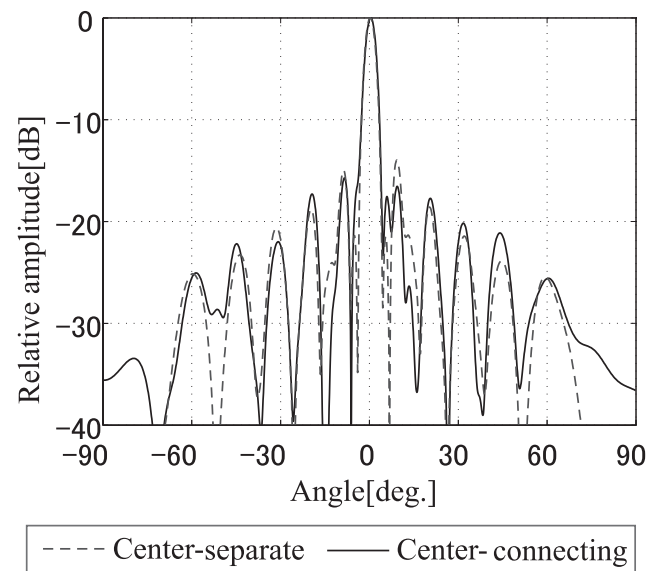


Fig. 21 Measured radiation patterns at 78 GHz.

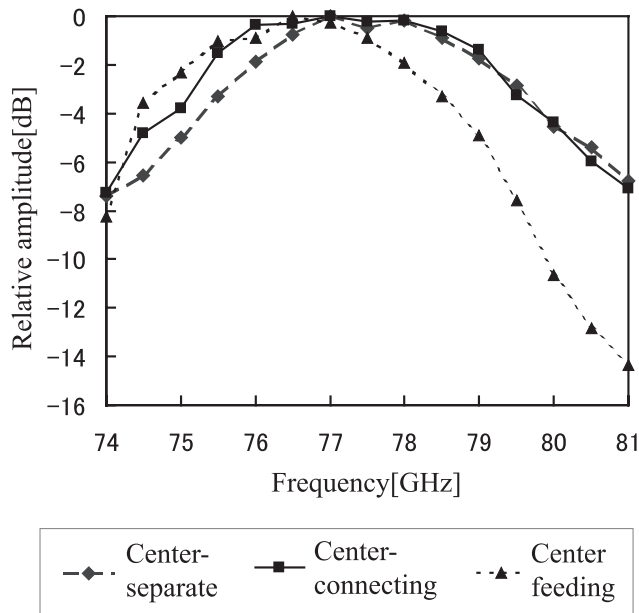


Fig. 22 Measured frequency dependency of gain.

pare the bandwidth. The bandwidths for the gain 3 dB lower than the peak level was 3.67 GHz for the center feeding, 3.94 GHz for the center-separate corporate-feeding and 4.25 GHz for the center-connecting corporate-feeding, which is 14% and 7% increasing from the center feeding and the center-separate corporate-feeding, respectively. Advantage for gain bandwidth of the center-connecting corporate feeding was confirmed by experiments.

6. Conclusion

The microstrip comb-line antennas with the waveguide corporate feeding system was developed in the millimeter-wave band. The feeding lines of the inner comb-line antennas were connected at their terminations. Therefore, matching elements are not necessary for these antennas. Furthermore, deviation of the aperture amplitude distribution fed from one side due to frequency change was compensated by the deviation of the distribution fed from the opposite side. Bandwidth of the antenna became broad. Four antennas with end feeding, center feeding, corporate feeding of center separate and corporate feeding of center connecting are compared to show the effect of the proposed antenna. The design of the antenna for the aperture Taylor distribution is presented with the design of the microstrip-to-waveguide transition for asymmetric power-dividing ratio and the waveguide circuit for corporate feeding. The bandwidth due to the aperture phase taper is evaluated by the array factor. The bandwidth due to the aperture amplitude distribution of the center-connecting antenna is evaluated by simulation and experiment of the two-end feeding antennas. The performance of the proposed antenna was evaluated and compared with the conventional antennas by electromagnetic simulations and experiments. The effect for the bandwidth of the radiation

pattern and the gain was confirmed.

References

- [1] D. Platt, L. Pettersson, D. Jakonis, M. Salter, and J. Hagglund, "Integrated 79 GHz UWB automotive radar front-end based on Hi-Mission MCM-D silicon platform," European Radar Conference EuRAD 2009, pp.445–448, Roma, Italy, Sept.-Oct. 2009.
- [2] H. Singh, J. Oh, C. Kweon, X. Qin, H. Shao, and C. Ngo, "A 60 GHz wireless network for enabling uncompressed video communication," IEEE Commun. Mag., vol.46, no.12, pp.71–78, Dec. 2008.
- [3] Y. Hayashi, K. Sakakibara, M. Nanjo, S. Sugawa, N. Kikuma, and H. Hirayama, "Millimeter-wave microstrip comb-line antenna using reflection-canceling slit structure," IEEE Trans. Antennas Propag., vol.59, no.2, pp.398–406, Feb. 2011.
- [4] M. Ando, Y. Tsunemitsu, Z. Miao, J. Hirokawa, and S. Fujii, "Reduction of long line effects in single-layer slotted waveguide arrays with an embedded partially corporate feed," IEEE Trans. Antennas Propag., vol.58, no.7, pp.2275–2280, July 2010.
- [5] Y. Ikeno, K. Sakakibara, N. Kikuma, and H. Hirayama, "Narrow-wall-slotted hollow-waveguide array antenna using partially parallel feeding system in millimeter-wave band," IEICE Trans. Commun., vol.E93-B, no.10, pp.2545–2553, Oct. 2010.
- [6] K. Seo, K. Sakakibara, and N. Kikuma, "Transition from waveguide to two microstrip lines with slot radiators in the millimeter-wave band," IEICE Trans. Commun., vol.E94-B, no.5, pp.1184–1193, May 2011.
- [7] K. Seo, W. Di, K. Sakakibara, N. Kikuma, and N. Inagaki, "K-band planar array antenna fed from transition between one waveguide and two microstrip lines," IEICE Technical Report, A-P2006-47, July 2006.
- [8] K. Sakakibara, D. Takagi, K. Seo, N. Kikuma, and H. Hirayama, "Bandwidth of multi-port microstrip-to-waveguide transitions in millimeter-wave band," International Symposium on Antennas and Propagation (ISAP2010), pp.119–122, Macao, Nov. 2010.
- [9] H. Iizuka, T. Watanabe, K. Sato, and K. Nishikawa, "Millimeter-wave microstrip line to waveguide transition fabricated on a single layer dielectric substrate," IEICE Trans. Commun., vol.E85-B, no.6, pp.1169–1177, June 2002.



Atsushi Kunita was born in Aichi, Japan, on June 15, 1986. He received the B.S. degree in Electrical and Electronics Engineering from Nagoya Institute of Technology, Nagoya, Japan, in 2009, and the M.S. degrees in electrical and computer engineering from Nagoya Institute of Technology, Nagoya, Japan, in 2011. He is currently working at ADVICS CO., LTD., Aichi, Japan.



Kunio Sakakibara was born in Aichi, Japan, on November 8, 1968. He received the B.S. degree in Electrical and Computer Engineering from Nagoya Institute of Technology, Nagoya, Japan, in 1991, the M.S. and D.E. degrees in Electrical and Electronic Engineering from Tokyo Institute of Technology, Tokyo, Japan in 1993 and 1996, respectively. From 1996 to 2002, he worked at Toyota Central Research and Development Laboratories, Inc., Aichi, and was engaged in development of antennas

for millimeter-wave automotive radar systems. From 2000 to 2001, he was with the department of Microwave Techniques in University of Ulm, Ulm, Germany, as a Guest Researcher. He was a lecturer at Nagoya Institute of Technology from 2002 to 2004, and is currently an Associate Professor. His research interest has been millimeter-wave antennas and circuits. Dr. Sakakibara is a senior member of IEEE.



Kazuyuki Seo was born in Okayama, Japan, on July 5, 1951. He received a B.S. degree in Electrical Engineering from Okayama University, in 1975. From 1985 to 2001, he worked at Kojima Press Industry Co., Ltd., in Aichi, and was engaged in the development of antennas for mobile communication systems. He has 21 years of industrial experience in automotive antennas. He is presently a Ph.D. student at the School of Computer Science and Engineering, Nagoya Institute of Technology. His research

interests are antennas for mobile communication systems and radar systems.



Nobuyoshi Kikuma was born in Ishikawa, Japan, on January 7, 1960. He received the B.S. degree in electronic engineering from Nagoya Institute of Technology, Japan, in 1982, and the M.S. and Ph.D. degrees in electrical engineering from Kyoto University, Japan, in 1984 and 1987, respectively. From 1987 to 1988, he was a Research Associate at Kyoto University. In 1988 he joined Nagoya Institute of Technology, where he has been a Professor since 2001. His research interests include adaptive and signal processing

array, multipath propagation analysis, mobile and indoor wireless communication, and electromagnetic field theory. He received the 4th Telecommunications Advancement Foundation Award in 1989. Dr. Kikuma is a senior member of the IEEE.



Hiroshi Hirayama received his B.E., M.E., and Ph.D. in Electrical Engineering from the University of Electro-Communications in Chofu, Japan, in 1998, 2000, and 2003, respectively. Since 2003 he has been with the Nagoya Institute of Technology, where he is currently a research associate. His research interests include signal processing techniques and EMC/EMI. Dr. Hirayama is a member of IEEE.